

Detailed study of tube hot rolling process by means of FEM

GARCÍA GIL Eduardo^{1,a,*}, DURÁN Gorka Llamazares^{1,b}, CONDE Aintzane^{1,c},
MURILLO-MARRODÁN Alberto^{1,d} and ATUTXA Jon Barco^{2,e}

¹University of Deusto, Avda. Universidades 24. 48007 Bilbao, Spain

²Tubos Reunidos Group, Barrio de Sagarribai, s/n 01470 Amurrio, Álava, Spain

^ae.garcia@deusto.es, ^bgorka.llamazares@opendeusto.es, ^caintzane.conde@deusto.es,
^dalberto.murillo@deusto.es, ^eJbarco@tubosreunidos.com

Keywords: Tube Rolling, Hot Forming, FEM Simulation

Abstract. In this paper seamless tubes hot manufacturing calibration rolling is studied by means of a finite element model, to improve product quality and process performance. Based on real data provided by an industrial partner, Tubos Reunidos Group, a finite element model of the process has been created and validated for the thermo-mechanical analysis of the process. The model has been used for the study of the wall thickness evolution and peripheral distribution during process, the eccentricity and the polygonization effects. Results show that the tube velocity in the process is one of the factors affecting wall thickness eccentricity, due to mass flow conservation. Regarding polygonization and eccentricity effect it has been found that both effects increase in the rolling stands with higher reduction ratio, and are corrected afterwards. These effects are mainly due to the ovality of the rolls. However, the effect the different sliding velocity along roll perimeter has implications in the local deformation of the material in contact with the roll, causing local compressive stress areas in addition to the predominant tension areas.

Introduction

The manufacturing of seamless pipes is a complex process in which high temperature, strain rates and forces are involved to achieve a high-quality product. Seamless pipes are used in severe environments applications, such as, refineries, transport of fluids under high pressures, oil drilling operations, etc. Usually, seamless tubes offer higher resistance and mechanical properties than welded pipes [1].

The manufacturing process of seamless tubes consists of three steps, piercing, elongation in mandrel mill and final rolling calibration. The three steps have influence on the quality and accuracy of the final product; however, in the last step the geometrical accuracy is given to product.

The efforts for improving the quality of the tubular products obtained with this process have been extended from the beginning of the process itself, as it can be seen in the research work of Vargas et al. [2]. However, the studies involving numerical models are more recent, mainly from the present century. In 2003, Bayoumi [3] developed a steady-state analytical model of the roll-pass geometry, which studied the effects of roll gap opening and the inter-stand velocity increase ratio in process parameters such as wall thickness, inter-stand tensions, roll load and rolling. The results showed that the interstand velocity increase ratio increased the inter-stand tension while the roll load remains almost unchanged. Carvalho et al. [4] modeled the process for the manufacture of seamless tubes both numerically and via hot torsion testing and predictions of final average ferrite grain sizes were given, with larger predictions for ferrite grains sizes, which were attributed to the assumptions made during the study.

The analytical models gave an interesting insight for the process; however, they were limited in terms of the accuracy of the results and the number of variables analyzed. Therefore, most of the recent works use the Finite Element Method, FEM, to simulate the process with a higher

accuracy and broader studies. The calculation power increase of computers and the improvements of the commercial software, has boosted the complexity of calculations and the results obtained.

The high accuracy demanded by final pipe users respond to the need to thinner but homogenous walls, free from residual stresses and superficial defects. Dimensioning of the tubes is based on the thinnest and, consequently, weakest section. Thus geometrical non-homogeneities such as eccentricity and polygonization lead to an increase in weight of material [5]. Accordingly, important research efforts have been dedicated to improve the geometrical accuracy of the final product. In fact, these effects are not exclusive of this rolling mill, since they can be generated even in piercing phase [6], and elongation in mandrel mill [7].

During the rolling of the tube its diameter is reduced progressively, higher reductions are performed in the initial boxes while lighter reduction occur at the end. In the rolling stands with greater reductions, the rolls have an elliptical shape to prevent material from jamming, which leads to polygonization of the tube. A study devoted to reduce polygonization [8] concluded that interstand tension and the correct selection of initial diameter are key factor for reducing this effect. Jiang et al. [9] developed a high precision FE model for predicting the defect of inner polygon. The model allowed the identification of the peak stress at the roll root contact area while the stress of the roll gap contact area was smaller, leading to a distribution of six stress peaks. These works pointed out the difficulties faced to obtain a proper and accurate Finite Element Model: material behavior constitutive model, contact and friction boundary conditions, and heat transfer.

Another aspect of interest is related to the tube eccentricity. Jiang et al. [10,11], designed a set of eccentric rolls which induced a moment on the tube causing it to rotate around its axis while it advances through the mill. In [10] the tube rotation method is presented for a single pass of the tube rolling process and analyzed by means of FEM, showing an improvement in the evenness of thickness distribution. Afterwards, in [11] the theory of the rotation is analyzed along with a FEM that is validated with experimental results. The rolling forces, torque, energy consumption are evaluated, from a process point of view, and the thickness, temperature and stress of the tube are studied from a product point of view. This technology is applied to thick steel tubes in a recent contributions of the authors [12].

In this paper a FEM model of the hot tube Sizing Mill, SM, of AISI 1016 has been developed based and validated with industrial data with the aim of fully understand the factors affecting the final geometry of the tube at the end of the process: wall thickness, eccentricity, and polygonization. Thanks to the model the reasoning for their occurrence, and alternatives to reduce its relevance have been obtained. The model has been also modified to evaluate the effect of typical alterations occurring in plant in the real process: pre-existing eccentricity, tube temperature heterogeneity, or roll misalignment.

Experimental Setup

In this study the calibration rolling of AISI 1016 steel is studied. Material composition % in wt. is presented in Table 1.

Table 1. Chemical composition of the AISI 1016 steel.

C	Si	Mn	Ni	P	S	Cr	Mo	Al	Cu
0.12 - 0.17	max 0.3	0.3 - 0.6	max 0.25	max 0.035	max 0.035	max 0.2	max 0.05	max 0.01	max 0.3

The calibration consists of seven driven stands of three rolls each, as it can be seen in Fig. 1, which are equally distributed to reduce the tube diameter from 200.50 mm to 180.80 mm. The disposition of the rolls in each box is rotated 60° from one box to another, giving as result that the groove of the rolls in the preceding box is the border of the rolls in the next, as shown in Fig. 1.

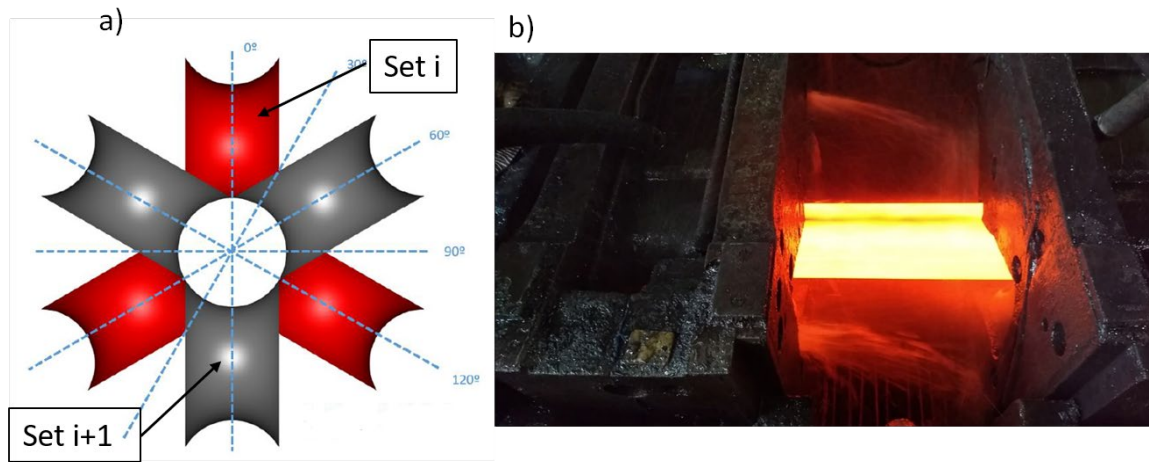


Fig. 1.a) Disposition of the rolls in the driven mill stand of two subsequent sets, where the rotation can be seen. B) Experimental image of the rolled tube passing between two driven stands.

Before entering rolling stands the material is reheated in a gas furnace to a temperature of 1020°C. Then the material is pushed into the SM and is driven by the rolls thanks to friction. According to the measurements recorded by Tubos Reunidos Group on shop the advanced mean velocity of the tube is 1018.9 mm/s. Fig. 1 b) shows the tube passing between two boxes. By contrast, the tangential velocity of the rolls varies along the mill from 876.5 mm/s in the first stand to 1124 mm/s in the last two stands. Accordingly, for the analysis of the process it is important to notice that the usual contact between the roll and the tube is sliding contact.

During the rolling of the tube the mean power consumed by the electric motors was 24 kW, and the mean temperature of the billet between stands was 980.43°C. After the process the final length of the tube was measured. Additionally, a tube was stopped in the middle of the process to measure its wall thickness between driven stands. For the thickness measurements, ten values have been acquired circumferentially equally distributed along tube perimeter using infrared IMS system. Results are used in section 4 for comparing experimental with numerical results.

Numerical Model

In this section the numerical model developed for the simulation of the SM is presented. The geometries of the different elements involving the mill were designed according to data provided by Tubos Reunidos Group separately using SolidWorks software and assembled together before being exported to Forge NxT®.

The model, Fig. 2, consists of seven rolling stands with 3 rolls in each stand, the tube or billet, a guide to lead the tube into the SM and a pusher used to feed the tube into the mill. For simplicity of the simulation, all tools were selected as non-deformable (rigid) objects with thermal properties and the billet (tube) was set as a deformable object with thermal properties. The tools were meshed with 2D triangular elements, while the billet was meshed with 3D tetrahedral P1+ linear elements with a bubble node, size factor of 0.7, volumic size factor of 2.2 and mesh size of 4 mm to achieve at least 3 elements on the tube initial thickness. The Hensel-Spittel constitutive law is chosen to model AISI 1016 behavior at different temperatures, strain, and strain rates. The materials coefficient were provided by the software and validated with the industrial partner [13]. The coefficients used are shown in Table 2.

Table 2. *Hansel-Spittel coefficients for AISI 1016.*

Coefficient	Value
A1	752.5394
m1	-0.00219
m2	-0.1523
m3	0.13792
m4	-0.0486

According to experimental data the initial temperature of the billet was set to 1020°C, and that of the rolls to 50°C. Heat transfer coefficient were set according to [14]. Regarding friction, based on [15] the viscoplastic or Norton law was selected for the contact between the rolls and the tube with a coefficient of 0.33, adjusted by curve fitting comparing experimental and numerical results, mainly velocity and power consumption.

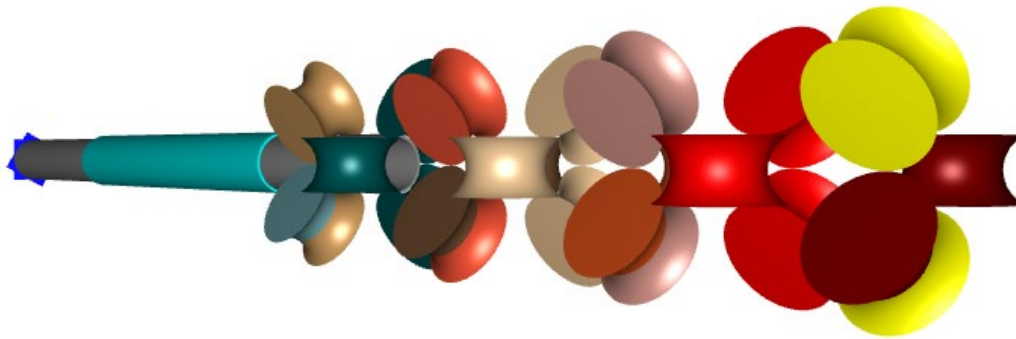


Fig. 2. *Geometrical disposition of the model with the tube and the 7 driven stand rolls.*

Results and Discussion

The results of the model are presented in this section along with the discussion of the main aspects obtained from the simulation.

For the validation of the numerical model the obtained results of power consumption, tube velocity evolution, temperature and tube thickness evolution and length increase are compared to experimental results. On the one hand the mean power obtained from the simulation is 28 kW, which is 16.7% higher than the experimental measurement, a result accurate enough result given the dispersion of experimental measurements done on-shop.

Billet velocity increases along the process from 968 to 1049 mm/s which agrees with the experimental measurements described in previous section.

The temperature evolution of the billet during the milling process is fairly constant both numerical and experimentally, being the difference of 4% between the experimental mean value (980.38°C) and the numerical one (1016.51°C).

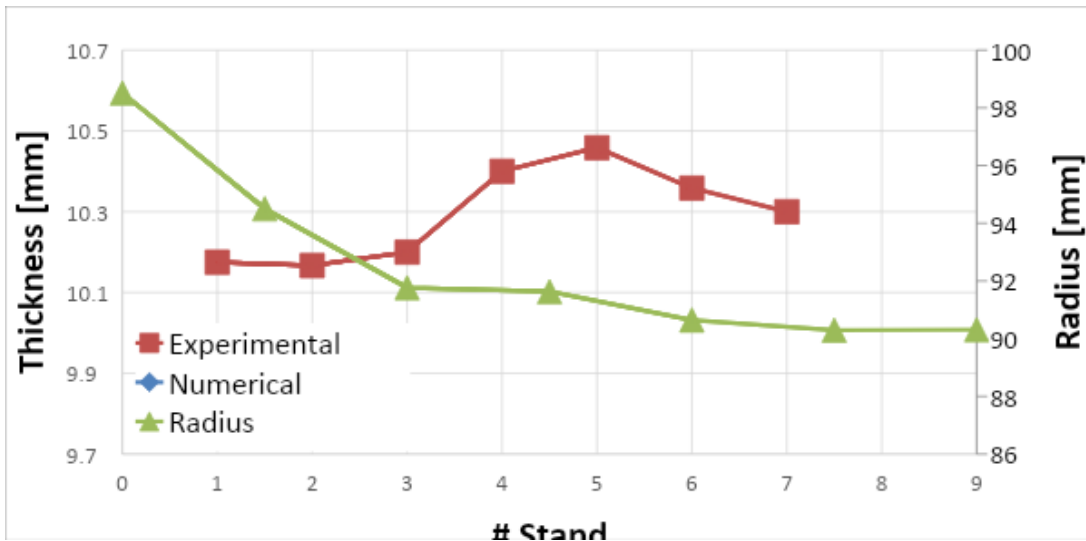


Fig. 3. Mean thickness evolution measured after each rolling stand. Experimental vs. Numerical.

Finally, the geometrical accuracy of the model is analyzed comparing the mean thickness evolution after each rolling stand. In Fig. 3 it can be seen that the agreement is good with a maximum deviation below 6%. Once the validity of the model has been justified, the model is used to study in detail eccentricity and polygonization effects during the process.

First the wall thickness increase is discussed. As in any plastic forming process, the volumetric flow rate must be kept constant during the rolling, (assuming that the density is constant). Accordingly, the diameter reduction must be accompanied with a length or/and thickness increase. In order to avoid the effect of thickness increase during the process, it would be necessary to adjust the billet velocity to keep the cross-section area constant while the diameter is reduced, for that the material velocity should be updated

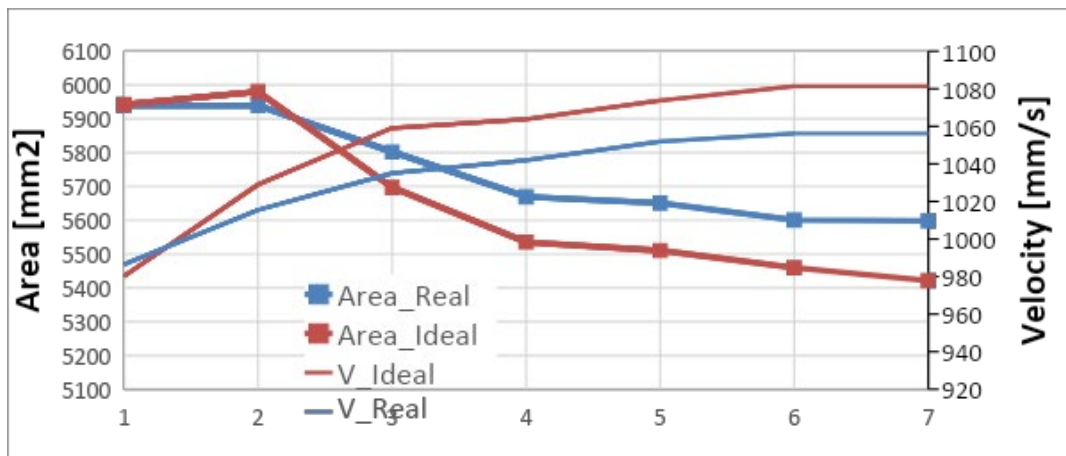


Fig. 4. Evolution of cross section area and tube velocity along the process. Real values are obtained from the model, and ideal values have been calculated to keep tube thickness constant.

From the model the real area after each rolling stand and the real velocity have acquired and they have been compared to the ideal area that would maintain the wall thickness constant, giving as a result the ideal velocity in each stand, that is, the velocity of the material that would make the wall thickness constant, results are shown in Fig. 4.

Results show that the velocity of the tube in the real process is lower than the ideal one, up to a 3% in the last stand. This analysis has not been found in literature, and it must be pointed out that the implementation of this solution in the industrial process would improve the quality of the product but a proper assessment of rolls velocity must be done to match the material flow given the effects of friction and sliding.

Fig. 5 shows the wall thickness evolution at different angles (0° , 30° , 60° , 90° , and 120°) (see Fig. 1) as well as the eccentricity evolution measured after each rolling step. Two interesting conclusions can be obtained from this graph.

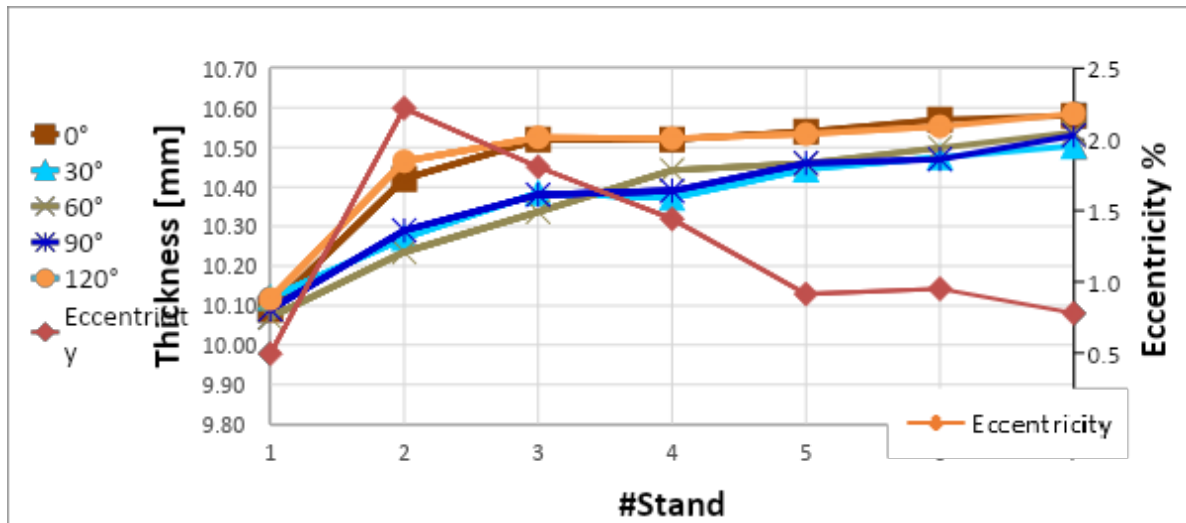


Fig. 5. Wall thickness evolution at different angles (0° , 30° , 60° , 90° , and 120°) and eccentricity evolution measured after each rolling stand.

On the one hand, it can be seen that the thickness evolution can be divided into 3 groups: group 1 involving 0° and 120° , group 2 with 30° and 90° , and 60° . The behavior of group 1 correspond to the planes that face the groove of the roll in the second stand, thus they experiment an important thickness increase. Group 2, instead, face the border of the roll at the second stand, leading to a smaller thickness increase. Finally, the plane at 60° is in the middle of the roll between the groove and the border. Looking at the eccentricity evolution it can be seen that it is at the stage of maximum difference between group 1 and group 2, that is in the second roll, that the eccentricity is higher. Then, as long as the lines trend to merge the eccentricity is reduced.

Thus, a clear relationship between the thickness evolution at circumferentially and the eccentricity is set. This difference is caused by the roll perimeter design, which is not circular but elliptical. It is also important to notice, that the biggest increase in eccentricity is generated in the rolls with the higher diameter reduction which are stands two and three, as shown in Fig. 3.

In order to fully understand the phenomena occurring at the contact between the rolls and the tube the sliding velocity and the longitudinal stresses of the tube are analyzed hereafter. Fig. 6 a) shows the relative velocity in the tube axial direction between the roll and the tube in the stand 3. There it can be seen that in the groove of the roll the material is moving faster than the roll, while in the corners of the roll it is the opposite: the tangential velocity of the roll is higher than the velocity of the tube. Fig. 6 b) shows the displacement of the material passing through the roll, where it is appreciated how the material is pushed forward in the area of the corner of the rolls, and it is retained in the groove of the roll, causing an undulated shape. This effect, which is due to the different diameter of the roll along its perimeter is enhanced by the roller's ovality. Moreover, it creates a stress-strain distribution which is depicted in Fig. 7 a) strain, and b) stress.

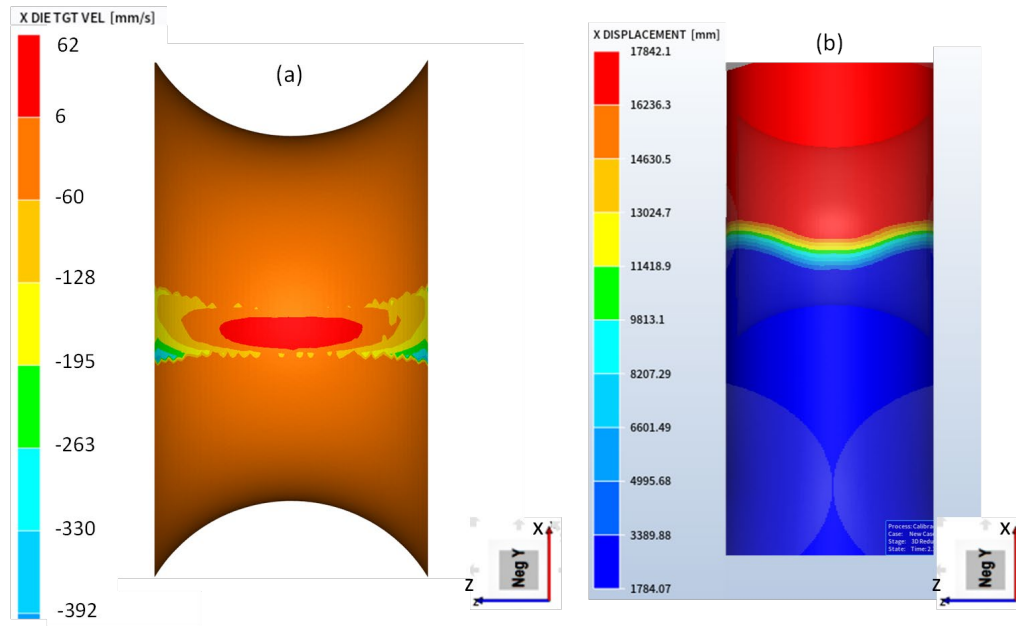


Fig. 6. a) Relative velocity between the roll and the tube in stand two. b) Tube material displacement at the pass of stand 3.

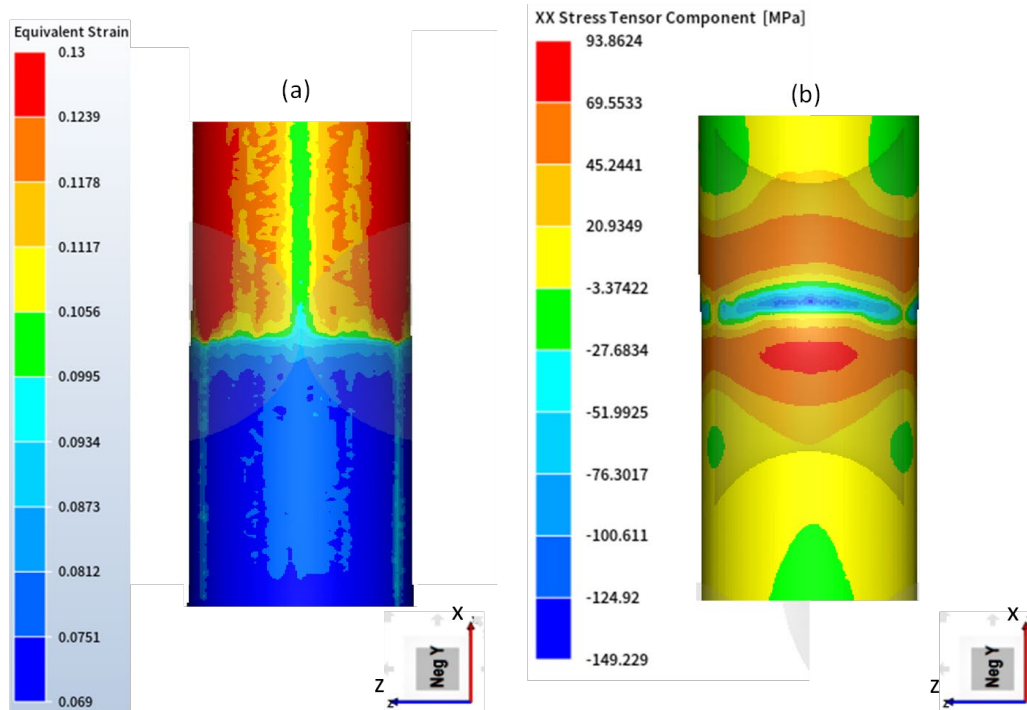


Fig. 7. a) Equivalent strain of tube material when passing through stand 3. b) Axial stress of the tube material in the surroundings of stand 3.

In Fig. 7 b) it can be seen that most of the tube is under tension stress (positive), which agrees with literature. However, in the contact region between the roll and the tube important compressive stresses are generated which are higher in the groove section and almost 0 in the corners of the roll. This finding has not been reported previously and is one of the reasons for the generation of eccentricity effect. The equivalent strain shown Fig. 7 a) confirms the difference in behavior between the central region in contact with the groove and the regions in contact with the border of

the roll. As above mentioned, the growing diameter of the roll along its wildness is responsible for this effect, and the ovality of roll's perimeter enhances the consequences.

Finally, the polygonization effect is addressed. It is related to the ovality of the rolls, which is high in the initial stands and reduced in the last ones. The evolution of this effect is shown in Fig. 8.

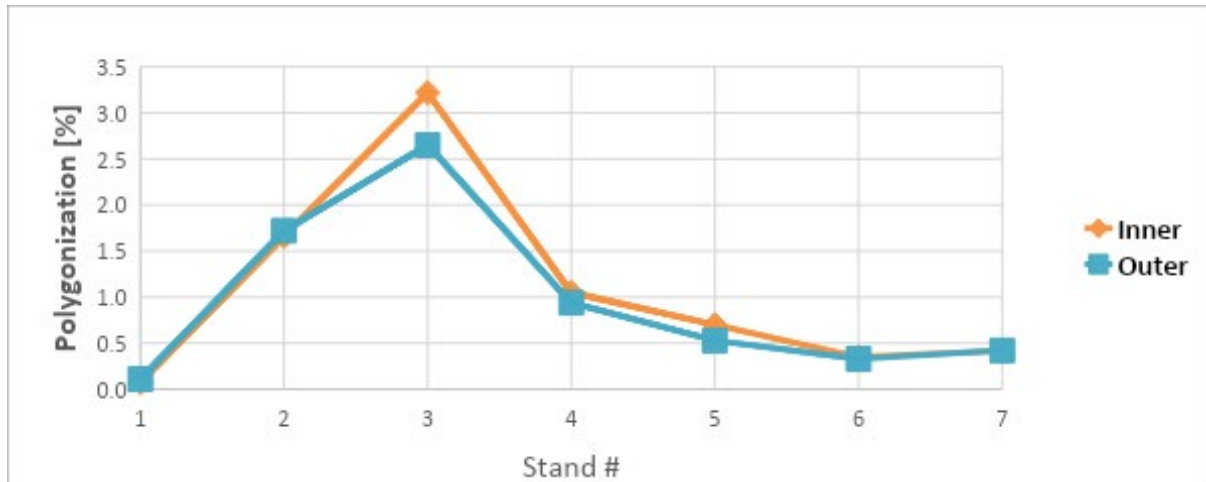


Fig. 8. Evolution of polygonization effect along the SM.

This effect increases from 0 at the beginning of the process to a maximum of 3.2% in stand number 3, where the maximum diameter reduction is done. Afterwards, the polygonization is reduced up below 0.5% at the end of the SM. This phenomenon is due to the ovality of the rolls, which flatten the tube passing over the groove of the roll. Since the ovality of the rolls decreases along the stands so does the ovality.

Finally, the radial deviation from the theoretical circular profile has been calculated in the cross section of the tube after each stand. Results are depicted in Fig. 9, the evolution of the radial deviation follows a sinusoidal trend with 3 positive peaks and 3 negative peaks, which represent the polygonization effect. These peaks are clearly relevant after stands 2 and 3, those with higher reduction and ovality, and consequently the higher polygonization of the tube in those positions. Then, in subsequent stands those peaks are flattened. This way it is illustrated how the tube profile is expanded in the corner of the roll ((positive and negative peaks) and flattened in the groove of the subsequent roll, due to the 60° rotated configuration is rotated 60° of the mill. This flattening effect of the rotated stands reduces progressively the big deviation created in stands 2 and 3, but the geometry is not fully corrected after stand 7.

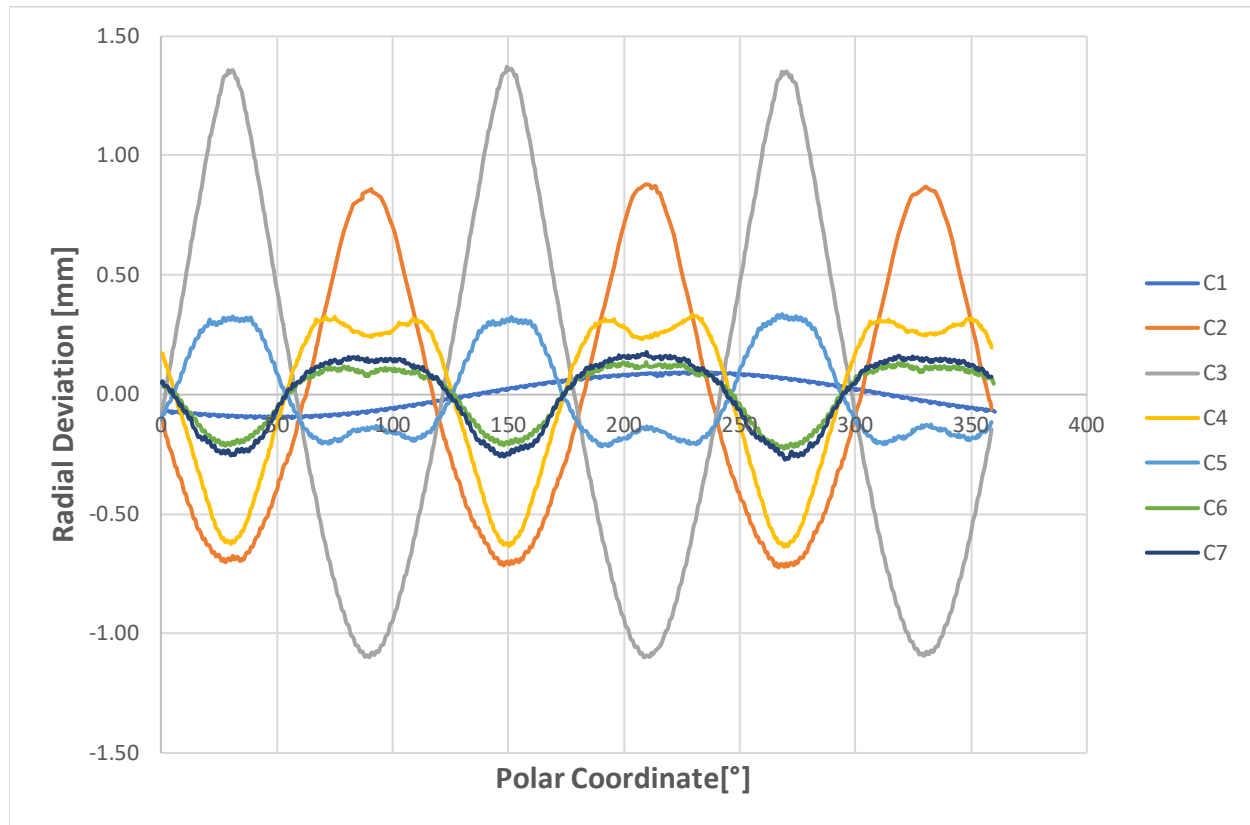


Fig. 9. Radial deviation of the tube along the periphery of the tube in each stand.

This polygonization is an undesired effect for tube produces and is due to the ovality of the roll's profile. Perfect circular rolls would strongly reduce this phenomenon; however, those type of roll profile could present limitations for material flow during rolling, according to actual experience.

Summary

In this paper the calibration rolling of seamless AISI 1016 tubes is deeply analyzed by means of a FEM validated thanks to experimental data provided by an industrial partner, Tubos Reunidos Group. From the work developed the following conclusions can be drawn:

- The effect of thickness increase is analyzed based on material flow. Results show that increasing tube velocity will help reducing this effect.
- The effects of eccentricity and ovality have been deeply assessed. Both effects increase between stands 2 and 3, and decrease progressively in the subsequent stands. The ovality of the rolls has been found to be the cause of both effects since it distorts the circularity of the tube.
- Process parameters such as relative velocity, material displacement, equivalent strain and axial tension are evaluated in the contact between the rolls and the material showing that the difference of tangential speeds along rolls perimeters leads to non-homogenous stress-strain states on tube material.

References

- [1] V. Gopinathan, O. Pawelski, V.C. Venkatesh, Effect of cold and hot rolling and normalising on the structure and properties of welded joints, *J. Mech. Work. Technol.* 1 (1978) 361-370. [https://doi.org/10.1016/0378-3804\(78\)90038-4](https://doi.org/10.1016/0378-3804(78)90038-4)

- [2] J.M. Vargas, C. Pagliano, F. Medina, F. Muratori, F. Paganin, J. Paiuk, Process Optimization for the Manufacturing of Seamless Steel Tubes in a Continuous Mandrel Mill and a Stretch Reducing Mill, *IFAC Proc.* 22 (1989) 147-153. [https://doi.org/10.1016/S1474-6670\(17\)53102-X](https://doi.org/10.1016/S1474-6670(17)53102-X)
- [3] L.S. Bayoumi, Analysis of flow and stresses in a tube stretch-reducing hot rolling schedule, *Int. J. Mech. Sci.* 45 (2003) 553–565. [https://doi.org/10.1016/S0020-7403\(03\)00047-X](https://doi.org/10.1016/S0020-7403(03)00047-X)
- [4] R.N. Carvalho, M.A.C. Ferreira, D.B. Santos, R. Barbosa, Simulation of the Process of Hot Rolling of Seamless Tubes, *Mater. Sci. Forum* 539–543 (2007) 4602-4607. <https://doi.org/10.4028/www.scientific.net/MSF.539-543.4602>
- [5] F. Foadian, A. Carradó, H. Palkowski, Precision tube production: Influencing the eccentricity and residual stresses by tilting and shifting, *J. Mater. Process. Technol.* 222 (2015) 155-162. <https://doi.org/10.1016/j.jmatprotec.2015.03.008>
- [6] A. Murillo-Marrodán, E. García, J. Barco, F. Cortés, Analysis of Wall Thickness Eccentricity in the Rotary Tube Piercing Process Using a Strain Correlated FE Model, *Metals* 10 (2020) 1045. <https://doi.org/10.3390/met10081045>
- [7] Z. Wei, C. Wu, A new analytical model to predict the profile and stress distribution of tube in three-roll continuous retained mandrel rolling, *J. Mater. Process. Technol.* 302 (2022) 117491. <https://doi.org/10.1016/j.jmatprotec.2022.117491>
- [8] K. Stefański, W. Kubiński, Diminishment of internal polygonization of tubes in hot stretch-reducing mill, *Metall. Foundry Eng.* 36 (2010) 21. <https://doi.org/10.7494/mafe.2010.36.1.21>
- [9] Y.-Z. Jiang, X.-J. Li, X.-P. Zhang, K.-F. He, G.-F. Bin, High Precision FE Modeling for Predicting Inner Polygon Defect of Hot Rolled Seamless Steel Tubes, *KSCE J. Civ. Eng.* 22 (2018) 4445–4453. <https://doi.org/10.1007/s12205-018-1014-6>
- [10] Y. Jiang, H. Tang, Method for Improving Transverse Wall Thickness Precision of Seamless Steel Tube Based on Tube Rotation, *J. Iron Steel Res. Int.* 22 (2015) 924-930. [https://doi.org/10.1016/S1006-706X\(15\)30091-1](https://doi.org/10.1016/S1006-706X(15)30091-1)
- [11] Y. Jiang, H. Tang, X. Zhang, Rotation mechanics and numerical simulation of hot rolling process under asymmetric rolls, *Int. J. Mech. Sci.* 151 (2019) 785-796. <https://doi.org/10.1016/j.ijmecsci.2018.12.006>
- [12] J. Yong-zheng, Z. Sheng-shuo, F. Zhi-gang, Application of asymmetric roll pass for improving roundness of ultra-thick steel tubes, *Int. J. Adv. Manuf. Technol.* 119 (2022) 3571-3581. <https://doi.org/10.1007/s00170-021-08456-7>
- [13] Tubos Reunidos Group n.d. <https://www.tubosreunidosgroup.com/es/home> (accessed December 8, 2022).
- [14] R. Langbauer, G. Nunner, T. Zmek, J. Klarner, R. Prieler, C. Hochenauer, Investigation of the temperature distribution in seamless low-alloy steel pipes during the hot rolling process, *Adv. Ind. Manuf. Eng.* 2 (2021) 100038. <https://doi.org/10.1016/j.aime.2021.100038>
- [15] A. Murillo-Marrodan, E. Garcia, F. Cortes, A Study of Friction Model Performance in a Skew Rolling Process Numerical Simulation, *Int. J. Simul. Model.* 17 (2018) 569-582. [https://doi.org/10.2507/IJSIMM17\(4\)441](https://doi.org/10.2507/IJSIMM17(4)441)